nature sustainability

Article

https://doi.org/10.1038/s41893-023-01128-2

Ocean alkalinity enhancement through restoration of blue carbon ecosystems

Received: 20 August 2022

Accepted: 19 April 2023

Published online: 29 May 2023

Check for updates

Mojtaba Fakhraee [1,2] ✉, Noah J. Planavsky [1,2] ✉ & Christopher T. Reinhard [3]

Blue carbon ecosystems provide a wide range of ecosystem services, are critical for maintaining marine biodiversity and may potentially serve as sites of economically viable carbon dioxide removal through enhanced organic carbon storage. Here we use biogeochemical simulations to show that restoration of these marine ecosystems can also lead to permanent carbon dioxide removal by driving ocean alkalinity enhancement and atmosphere-to-ocean CO_2 fluxes. Most notably, our findings suggest that restoring mangroves, which are common in tropical shallow marine settings, will lead to notable local ocean alkalinity enhancement across a wide range of scenarios. Enhanced alkalinity production is linked to increased rates of anaerobic respiration and to increased dissolution of calcium carbonate within sediments. This work provides further motivation to pursue feasible blue carbon restoration projects and a basis for incorporating inorganic carbon removal in regulatory and economic incentivization of blue carbon ecosystem restoration.

Realistic trajectories that limit global average surface warming since the start of the industrial period to well below 2 °C require sustained atmospheric CO_2 removal together with massive and rapid reductions in global CO_2 emissions[1]. Natural modes of CO_2 removal, such as afforestation/reforestation and restoration of coastal habitats, have received considerable attention as potential carbon capture approaches given that they can also provide notable economic and ecological co-benefits[2,3]. For instance, through efficient conversion of atmospheric CO_2 to organic biomass followed by carbon burial in sediments, blue carbon ecosystems (BCEs) including mangroves and seagrasses have the potential to considerably enhance organic matter storage. Critically, BCE restoration also improves water quality, enhances marine biodiversity and ecosystem stability, provides a clear benefit to the health of coastal fisheries and can lead to a substantial reduction in storm damage to high-risk coastal communities[4,5].

BCEs cover only ~0.5% of the sea floor, but due to rapid rates of carbon sequestration in these ecosystems, they may contribute up to half of the organic carbon buried in ocean sediments on a global scale[6,7]. However, BCEs can also sequester or release CO_2 by shaping local carbonate chemistry (for example,refs. [8,9]). High organic matter input in BCEs can result in an increase in the rate of aerobic and anaerobic respiration (for example, sulfate reduction) with impacts on sedimentary pools of CO_2, porewater pH profiles, and reservoirs of alkalinity and dissolved inorganic carbon (DIC)[10–13]. Increased rates of alkalinity production within marine porewaters can lead to increased marine CO_2 uptake and capture of legacy anthropogenic carbon in the ocean, with a storage timescale that is effectively permanent (>1,000 years; for example, refs. 9,11,14). Although there has been increasing work on the export of alkalinity from shallow marine ecosystems[9,10,15–17], there has not been a systematic evaluation of the potential extent of increased alkalinity export likely to accompany BCE restoration. Further, enhancing carbonate precipitation—which leads to a drop in marine pH—can also drive marine CO_2 outgassing[8]. Herein, we use a stochastic modelling approach to show that, under a wide range of settings and conditions, restoring seagrass and mangrove ecosystems will reshape benthic marine redox dynamics in a manner that will drive ocean alkalinity enhancement (Fig. 1). We argue that this is an underappreciated aspect of the effects of BCE restoration[10,12], and one that makes the process a more robust and fungible form of CO_2 removal.

To investigate the potential role of mangroves and seagrasses in driving the permanent capture of anthropogenic CO_2 by enhancing benthic alkalinity fluxes, we built a time-dependent model of marine

[1]Department of Earth and Planetary Sciences, Yale University, New Haven, CT, USA. [2]Yale Center for Natural Carbon Capture, New Haven, CT, USA. [3]School of Earth and Atmospheric Sciences, Georgia Institute of Technology, Atlanta, GA, USA. ✉e-mail: mojtaba.fakhraee@yale.edu; noah.planavsky@yale.edu

https://doi.org/10.1038/s41893-023-01128-2

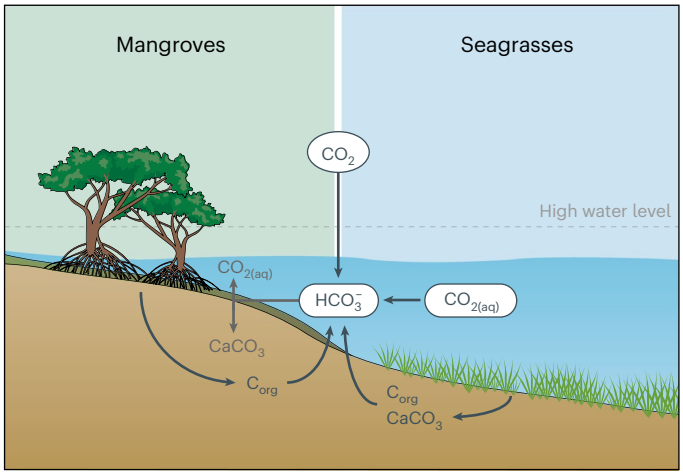

Fig. 1 | The blue carbon benthic alkalinity pump. The release of organic matter and nutrients from the roots of mangroves and seagrasses results in higher rates of aerobic respiration near the sediment–water interface and increases carbon flow through anaerobic microbial metabolism, both of which lead to a net increase in benthic alkalinity fluxes to the overlying shallow ocean. These alkalinity fluxes drive re-equilibration of the seawater carbonate system, which sequesters anthropogenic carbon from the atmosphere and shallow ocean for timescales of ~10^5 years.

sediment biogeochemistry that simulates the cycling of carbon, nitrogen, iron and sulfur under a wide range of environmental conditions. The model is designed to represent seagrass and mangrove environments but builds from well-established practices of modelling marine sediment biogeochemistry[18]. Production of alkalinity from anaerobic respiration (for example, sulfate reduction) and dissolution of calcium carbonate due to changes in redox structure are emergent features of the model. The model also tracks the acidity production resulting from the oxidation of reduced species (for example, sulfide), to ensure that the effects of BCE restoration on local carbonate chemistry are as representative as possible. Lastly, we also include advection (by plants, bioturbating animals and tidal pumping) and biological production of methane through organic matter degradation and consumption of methane through the aerobic and anaerobic oxidation pathways.

Our biogeochemical model is validated against measured depth profiles of key solid and dissolved phases in multiple extensively studied modern seagrass and mangrove systems (Supplementary Figs. 1–5). The model successfully captures observed depth profiles of oxygen, DIC, alkalinity and pH in a seagrass site in the Bahamas[12] with limited calibration (using observed ranges for all boundary conditions), for cases with and without seagrass. The model is also calibrated against measurements made in multiple mangrove sites[19,20], and successfully reproduces the depth profiles of oxygen, sulfide, pH and total organic carbon (TOC) in two different mangrove habitats. The organic matter flux from mangroves and seagrasses (rootzone fluxes) is highly variable and represents the only parameter used to tune the model to observed profiles. However, the inverted range of organic matter fluxes falls within the reported ranges for these regions (for example, ref. 2) and ranges used in our stochastic simulations (see below). The results of the calibration for both seagrass and mangrove sites are shown in Supplementary Figs. 1–5.

We use a stochastic approach in which environmental conditions and key model parameters are randomly varied within reasonable observational ranges, yielding a statistical estimate of the increase in benthic alkalinity flux expected during the restoration of BCEs across a range of scenarios (see section Time-dependent sediment diagenesis model; Methods and Supplementary Information). In the stochastic simulation, the modeled input parameters (for example, reaction rate constants and organic and inorganic burial fluxes), and boundary conditions (for example, bottom water DIC and alkalinity) were varied to better account for variability in environmental conditions across a range of seagrass and mangrove settings. We also varied the extent of advection, which in BCEs is caused mainly by bio-irrigation and tidal pumping (for example, ref. 21). The model input parameters were varied within the range suggested in the literature (Supplementary Table 3), assuming a uniform distribution (log-uniform for parameter ranges that span multiple orders of magnitude). The stochastic analysis was conducted for cases with and without allochthonous, pre-formed carbonate to assess the role of carbonate dissolution in replenishing the sedimentary alkalinity pool.

We estimate potential carbon dioxide removal based on the difference between the total benthic alkalinity flux before and after seagrass or mangrove restoration, assuming a CO_2 uptake efficiency between 75% and 85%. Mechanistically, benthic alkalinity fluxes sourced from mangrove or seagrass sediments will lead to an imperfect translation into an increased air–sea flux of CO_2, owing to the buffering capacity of surface ocean waters[22–24]. The magnitude of this effect is controlled by the thermodynamics of the carbonic acid system (and thus seawater temperature and salinity) as well as the existing state variables of the local carbonic acid system and the kinetics of air-sea gas exchange. We estimated the impact of this effect using an uptake efficiency for CO_2 removal (δCO_2) which is a function of changing net alkalinity[22–24] (δALK; alkalinity increases after carbonic acid system re-equilibration once alkalinity and DIC leave the sediment pile) (Fig. 2; see section 3; Methods and Supplementary Information). We emphasize that these values are only approximate, as they assume thermodynamic equilibrium and fully equilibrated air-sea gas exchange.

Results

Our modelling results indicate that in essentially all conditions mangrove and seagrass restoration will notably enhance alkalinity production in the sediment, leading to surface water alkalinity enhancement and uptake of CO_2 from the atmosphere. Restored mangrove and seagrass ecosystems cause a shoaling of oxygen penetration in the sediment and increased alkalinity production through anaerobic respiration. Mangroves and seagrasses deliver more organic matter to sediments under similar conditions relative to degraded marine ecosystems that represent a baseline before a given restoration project—the core idea behind BCE driving increased organic carbon burial. This shift in organic matter loading and marine sediment redox structure results in elevated alkalinity production and, critically, an increase in the flux of alkalinity from sediments into the overlying water column. Further, with a high concentration of pre-formed calcium carbonate (found in many mangrove environments, for example, the Bahamas[12] or the Red Sea[10]), there is an increase in the rate of calcium carbonate dissolution. Mechanistically, carbonate mineral undersaturation results from more localized and intense zones of acidity production, linked foremost to a zone of sulfide oxidation[12,13] in the presence of robust seagrass and mangrove growth. By increasing oxygen availability through the root zone and overall organic matter availability, seagrass and mangroves foster a higher rate of aerobic respiration as well as higher rates of sulfide oxidation relative to the unrestored baseline, which in turn results in increased acidity production in the surface sediment. A higher rate of acidity production decreases pH, resulting in a sharp decrease in the saturation index of calcium carbonate (Fig. 3). This effect is consistent with a sharp shift in the pH depth profiles in seagrass and mangrove systems (for example, refs. 10,12). However, despite a zone of more intense acid production—which can drive carbonate dissolution—the net effect relative to baseline scenarios is the transport (diffusion and advection) of waters with more alkalinity that will foster CO_2 uptake into the surface oceans.

It is important to assess the possibility that seagrasses and mangroves act as a source of CO_2 rather than a sink. Sulfate reduction can lower sediment pH, which could foster CO_2 evasion while increasing the alkalinity and DIC in the system. However, this effect is explicitly accounted for in our model framework. Further, these ecosystems

https://doi.org/10.1038/s41893-023-01128-2

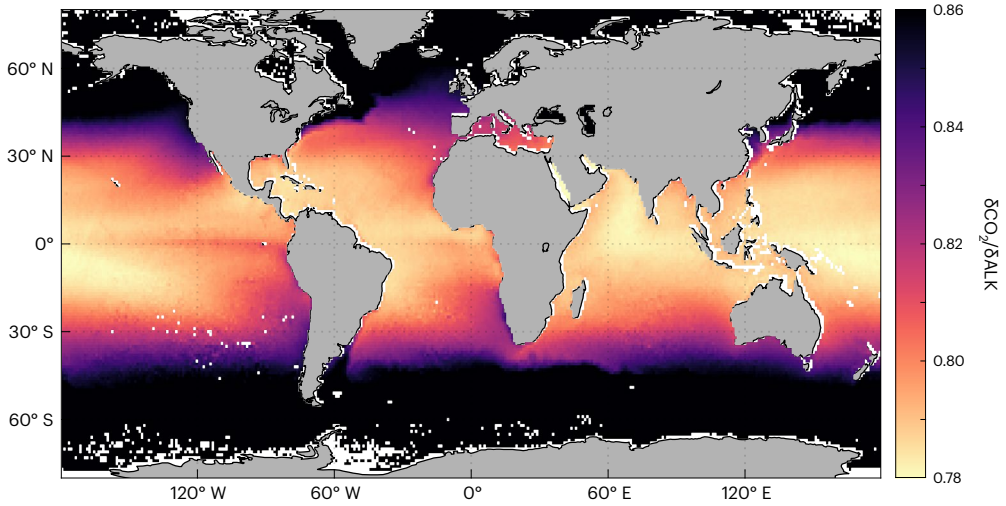

Fig. 2 | Surface ocean uptake efficiencies. Surface ocean uptake efficiencies ($\delta CO_2/\delta ALK$) based on WOA2018 temperature and salinity data and a re-equilibration of the carbonic acid system to alkalinity injection (see section Surface ocean response to benthic alkalinity enhancement; Methods and Supplementary Information).

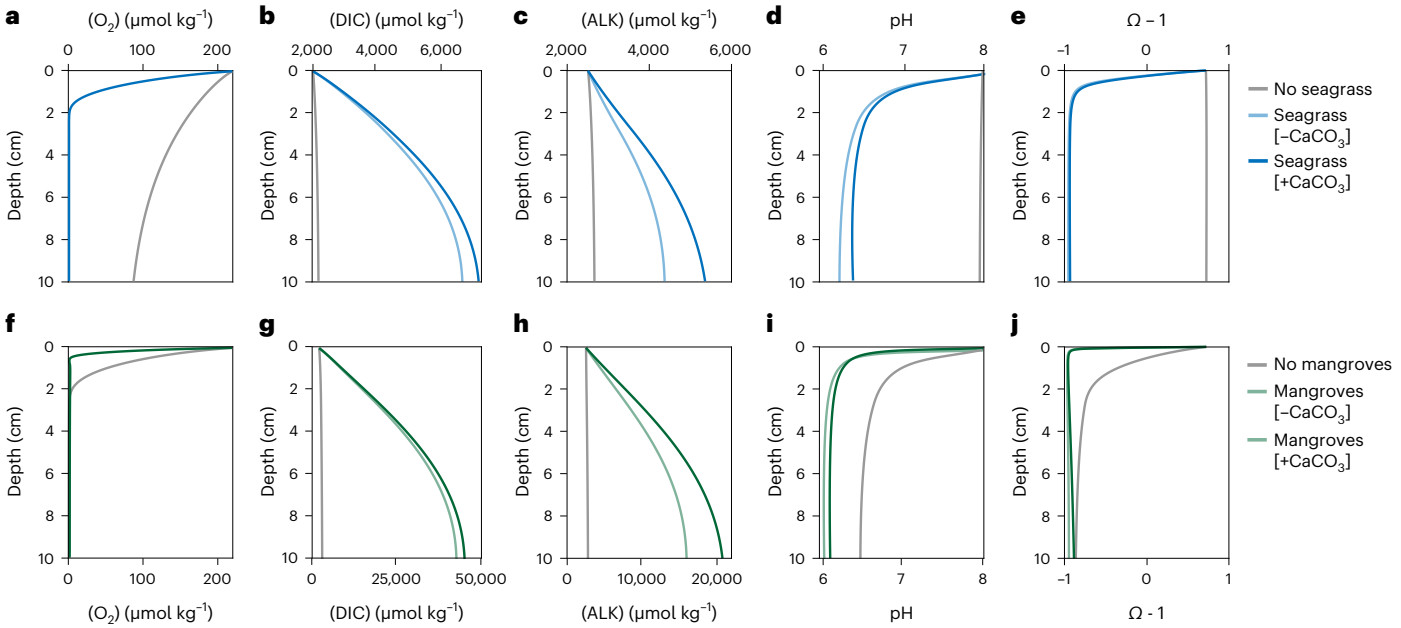

Fig. 3 | Modelled depth profiles of various chemical species in seagrass and mangrove sediments. The depth profile is for a baseline condition with bottom seawater chemistry. **a**–**j**, The depth profiles of dissolved oxygen, dissolved inorganic carbon (DIC), alkalinity (ALK), pH and carbonate saturation index for seagrass and mangrove systems. Our results suggest that seagrass and mangroves influence the organic and inorganic cycling of carbon in sediment, with strong impacts on diffusive alkalinity fluxes. In carbonate-rich sediment, seagrass and mangroves foster carbonate dissolution, resulting in increased alkalinity production. Through higher rates of carbon delivery and organic matter recycling mangroves produce a larger sedimentary alkalinity pool, emphasizing their potentially important role in alkalinity-based carbon capture.

can be a permanent sink of atmospheric CO_2 when the production of alkalinity from the sediment outcompetes the local rate of calcification (also potentially linked to restoration). The alkalinity production itself is a function of multiple environmental parameters including, but not limited to, the availabilities of organic matter and electron acceptor for anaerobic respiration (for example, iron oxides and sulfate), and the rate of sedimentary carbonate dissolution. Previous results have concluded that, under limited alkalinity production and probably high rates of local calcification in the water column, seagrass ecosystems can potentially act as a source of CO_2 (ref. 8). However, the high carbonate content in these ecosystems in many cases is due to the 'trapping' of carbonate from elsewhere ('allochthonous' carbonates; see, for example, ref. 11). Our results from an ecosystem budget analysis suggest that, for almost all cases, the rate of alkalinity production in these ecosystems is higher than rates of local calcification, making seagrass and mangrove ecosystems a net sink for CO_2 (Supplementary Fig. 10; see Supplementary Information).

Alkalinity-driven carbon capture by seagrass and mangroves

Our model analysis suggests that restored seagrass meadows can drive rates of atmospheric CO_2 uptake between 0.1 and 0.9 $tCO_2\ ha^{-1}$ per year, depending on the background rate of net primary production (Fig. 4). In systems with high background calcium carbonate concentration, the dissolution of calcium carbonate can considerably increase potential

https://doi.org/10.1038/s41893-023-01128-2

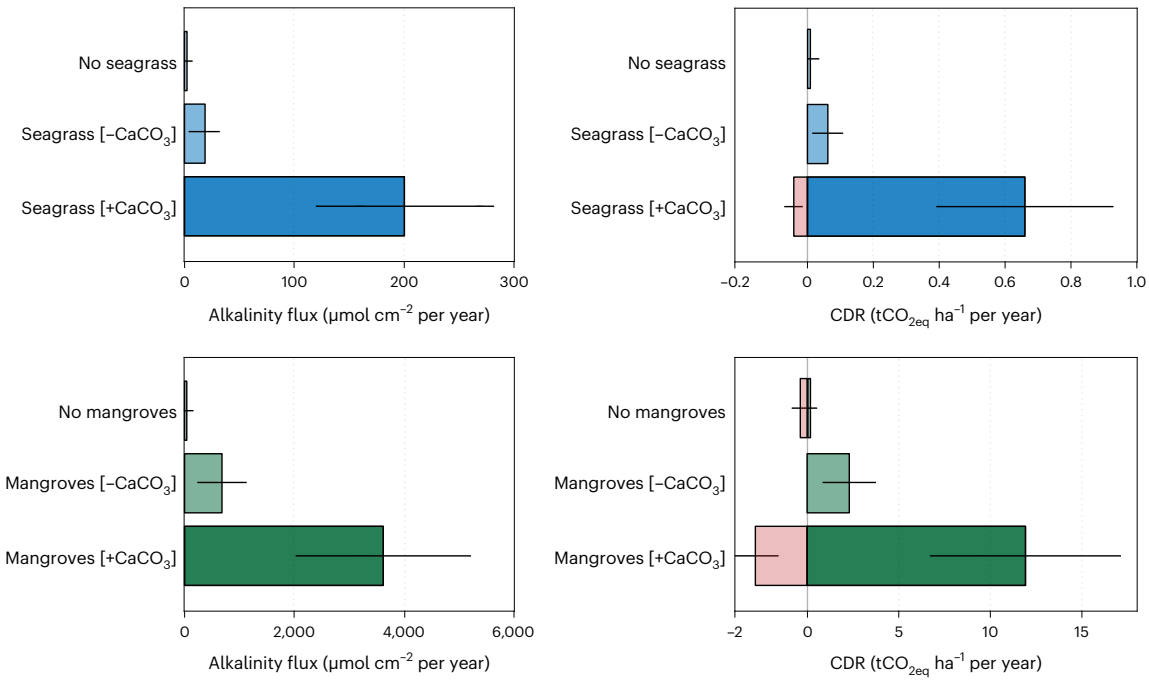

Fig. 4 | Regulation of greenhouse gas fluxes through the restoration of mangrove and seagrass ecosystems. Model results from our stochastic analysis (1,000 simulations) of changes to net alkalinity fluxes (left) and estimated area-normalized carbon dioxide removal (CO_2 removal; right) with and without seagrass (top) and mangrove (bottom) restoration. The red bars at right show offsetting methane (CH_4) fluxes estimated for the seagrass restoration and mangrove cases. CO_2 removal estimates are corrected for surface ocean buffering characteristic of the tropical/subtropical surface ocean (Methods and Supplementary Information). Error bars correspond to $\pm\sigma$.

CO_2 removal (up to ~0.9 tCO_2 ha^{-1} per year) (Fig. 4). The theoretical restoration potential of seagrass ecosystems is suggested to be between ~8 and 25 million ha (ref. 2), with the result that the alkalinity enhancement associated with extensive seagrass restoration could potentially remove between ~0.8 and 23 $MtCO_2$ per year.

The potential for ocean alkalinity enhancement and CO_2 capture in restored mangrove systems is notably larger than that of seagrasses, owing to the higher rate of organic matter release and trapping in mangrove systems relative to the background state. Stochastic analysis of our model yields an estimated CO_2 removal potential of ~1–17 tCO_2 ha^{-1} per year (Fig. 4), which when combined with an estimated theoretical mangrove restoration potential of ~9–13 million ha (ref. 2) yields an estimated CO_2 removal potential from restoration-induced alkalinity enhancement of ~9–221 $MtCO_2$ per year. Placed in the context of global CO_2 emission, our results collectively suggest that alkalinity enhancement driven by the restoration of mangrove and seagrass systems could permanently capture roughly 1% of total fossil fuel CO_2 emissions[25]. However, this is likely a theoretical upper limit on carbon dioxide removal, and it is important to emphasize that economic and societal pressures will make fully achieving this number extremely difficult. On the other hand, salt marshes should also drive marine atmospheric CO_2 uptake, and our model can also reproduce geochemical profiles in salt marsh sediments with limited tuning (Supplementary Fig. 3). Therefore, future work should focus on evaluating the CO_2 removal potential of marsh restoration.

Full greenhouse gas budget

Our results also suggest a relatively minor impact of benthic methane (CH_4) flux in offsetting CO_2 removal. Mechanistically, increased organic matter availability and decreased sediment oxygen penetration would be expected to lead to enhanced rates of biological CH_4 production (for example, ref. 26), which is consistent with our modelling results (Fig. 4). However, our results suggest that in typical cases the CO_2 equivalent flux from enhanced CH_4 production is small compared with the potential net increase in benthic alkalinity flux (Fig. 4). Although we have not explicitly modelled nitrous oxide fluxes, these have been shown to be a relatively small portion of the greenhouse gas budget in BCE systems[27–29].

Discussion

BCE restoration as permanent CO_2 removal

Carbon dioxide capture through benthic alkalinity enhancement represents durable (>1,000 years) CO_2 removal. This is in marked contrast to CO_2 capture through organic carbon burial, which can be rapidly remobilized in storm events or due to changes in coastal management practice[30]. Indeed, only a fraction of organic matter sequestered BCE escapes sedimentary recycling—most is converted into DIC (Supplementary Fig. 10). The degree to which the recycled carbon translates into permanent CO_2 removal is governed by the balance between the rate of alkalinity production through carbon recycling and the rate of alkalinity consumption, which themselves are a function of various environmental factors such as the local rate of calcification, availability of organic matter, and electron acceptors for anaerobic respiration (for example, iron oxides and sulfate). Seagrass and mangrove ecosystems can only be a permanent sink of atmospheric CO_2 when the production of alkalinity from the sediment outcompetes the local rate of calcification (Supplementary Fig. 10; see Supplementary Information). The most important outcome of our stochastic analysis is that this should be the case in essentially all BCE restoration projects. As a result, restoration of BCEs has the potential to lead to durable CO_2 removal regardless of uncertainty in the magnitude of CO_2 capture through conventional organic carbon burial.

Impacts of environmental stressors on CO_2 removal prediction

Synergistic environmental stressors associated with ongoing anthropogenic disruption might impact the potential ability of mangroves and seagrasses to capture carbon through benthic alkalinity flux enhancement. Despite gaps in knowledge regarding the impact of environmental stressors such as high seawater surface temperature, ocean acidification and eutrophication, there is evidence to suggest that

these factors may sustain or even increase the potential for alkalinity production in BCEs. For instance, available data suggest that increased surface seawater temperature, ocean acidification and eutrophication can augment rates of carbon sequestration by mangroves and seagrasses, which should also result in increased organic matter delivery to sediments and an enhancement of diffusive alkalinity fluxes. In addition to an increase in alkalinity-driven carbon capture, by modulating regional carbonate chemistry and thermodynamic buffering in coastal waters mangroves and seagrass can also act as an ideal natural means to mitigate the adverse effects of climate change on other coastal habitats (see section Synergistic environmental stressors on seagrasses and mangroves; Supplementary Information). Taken together, while our results emphasize the need to consider alkalinity fluxes in BCE restoration, the range of predicted CO_2 removal rates in different ecosystems also highlights the difficulty in moving CO_2 removal through enhanced alkalinity fluxes onto a carbon market. Nonetheless, it could be possible with a coupled modelling and empirical approach to estimate CO_2 removal rates and uncertainties from BCE restoration projects, and this represents a key target for future work.

Restoration costs of seagrass and mangroves

The potentially high cost of seagrass and mangrove restoration and maintenance represents a barrier to the robust growth of a blue carbon market, despite the obvious societal and ecological co-benefits[2]. Full restoration costs for previous mangrove and seagrass restoration projects can be as high as 100,000 USD ha^{-1}(ref. 3). Most of this cost is maintenance and monitoring of the project after its completion to ensure survival and reproducibility[31,32]. The restoration of seagrass is generally viewed to be labour-intensive and requires several years for the full completion of the project[31,32]. However, restoration of mangrove systems is typically more cost effective[3], with a median cost of restoration of ~1,000 USD ha^{-1}(ref. 3). However, the cost of mangrove restoration can be as low as 25 USD ha^{-1} per year (ref. 3). In this light, alkalinity-based CO_2 removal associated with mangrove and/or seagrass restoration could potentially offset a sizable fraction of the overall cost of many restoration projects. For instance, at a nominal carbon price of 100 USD tCO_2^{-1} alkalinity-based CO_2 removal alone would offset costs of up to 200–1,200 USD ha^{-1} annually for the restoration/maintenance of mangrove ecosystems.

Although there is increasing acceptance that CO_2 removal is going to be essential to meet climate goals, all proposed approaches towards CO_2 removal have drawbacks associated with energy use, cost, attribution, barriers to scale, and potential negative side effects (for example, refs. 33,34). Although the overall CO_2 removal ceiling for blue carbon systems is modest relative to other commonly discussed CO_2 removal approaches[35], seagrass and mangrove restoration is arguably unique as a CO_2 removal technique in that there are clear positive benefits for local communities and marine health from restoration and no obvious negative consequences. We argue that enhanced alkalinity generation has been overlooked (see also refs. 10,12) when accounting for carbon removal during the restoration of BCEs and suggest that a focus on the impacts of BCEs on the shallow ocean alkalinity budget provides an avenue towards financial incentivization of the restoration and protection of these critically important shallow marine ecosystems.

Methods

Time-dependent sediment diagenesis model

The vertical distributions of chemical species in the solute and solid phases within the sediment column can be expressed using the following reaction-transport formulation:

$$\frac{dC_i}{dt} = \frac{\partial}{\partial x}(\varphi D_i \frac{\partial C_i}{\partial x}) - \frac{\partial}{\partial x}(\varphi v C_i) + \varphi \alpha_{irr}(C_i - C_i^{burr}) + \varphi \sum_j R_{ij}, \quad (1)$$

$$\frac{dC_i}{dt} = \frac{\partial}{\partial x}(\psi D_b \frac{\partial C_i}{\partial x}) - \frac{\partial}{\partial x}(\psi u C_i) + \psi \sum_j R_{ij}. \quad (2)$$

Here, equation (1) refers to solute (dissolved) species, equation (2) refers to solid species, x is depth below the sediment–water surface, C_i is the concentration of species i, and D_i and D_b are respectively the corresponding molecular diffusion and bio-diffusion coefficients. The parameters u and v are burial velocities for solid and dissolved (advective) species. The parameter v represents the effect of all advective fluxes including the effect of tidal pumping, which is viewed to be a common feature of BCEs.

The parameter α_{irr} denotes the bio-irrigation coefficient. The parameter ψ is $(1-\varphi)\rho$, where φ and ρ are respectively the sediment porosity and density of dry sediment. R_{ij} corresponds to the sum of all the rates of reactions that consume or produce species i. Reactions, rate expressions and model parameter values, along with model initialization, boundary conditions and calibration to empirical observations, are described in section 1 of Supplementary Information.

Organic matter degradation

To account for the role of seagrasses and mangroves in increasing the concentration of oxygen and dissolved organic carbon (DOC) in porewater, we considered the transformation of particulate organic carbon (POC) to DOC and from DOC to DIC. The rate of organic matter transformation to DOC is a function of the abundance and reactivity of organic matter. Mechanistically, upon the burial of POC in the sediment column, POC (for example, biopolymers) with high molecular weights (HMW; ≫1,000 Da) would be broken down and depolymerized into smaller organic molecules with lower molecular weights (for example, DOC). The resultant DOC is then further degraded and mineralized, which results in the generation of inorganic carbon (DIC). The overall rate of carbon transformation from POC to DIC is controlled by the rate of each degradation step. While the mechanisms controlling the rate of the multi-stage conversion of organic matter to inorganic carbon are not fully understood, we use a well-established power-law framework for organic matter degradation. Using this power-law function for the carbon degradation rate, the rate of POC transformation into DOC can then be expressed as:

$$R_{POC-DOC} = k[OC]. \quad (3)$$

Here $R_{POC-DOC}$ denotes the rate of organic matter degradation, k is the reactivity of organic matter and [OC] is the concentration of POC. Following the previous studies, the reactivity, k, was described by the Middelburg power law as a function of carbon age t: $\log_{10} k = -(0.95)\log_{10} t - (0.81)$ (ref. 36). This power law was corrected for the effect of oxygen, which we used in the model and was shown to hold over a range of conditions[37].

Since the rate of the terminal mineralization step, where DOC is converted to DIC, is a function of both the size and reactivity of the POC pool, the rate of DOC to DIC transformation can be expressed by a Monod scheme. Such formulation is supported by experimental and modelling studies:

$$R_{DOC-DIC} = R_{POC-DOC} \cdot \frac{[DOC]}{k_{DOC} + [DOC]}, \quad (4)$$

where $R_{POC\text{-}DOC}$ is the rate of conversion of POC to DOC, calculated using the power law described above; [DOC] is the concentration of DOC; and k_{DOC} is the half-saturation constant for DOC degradation. The value of k_{DOC} has been suggested to be approximately 231.16 ± 899.99 μM (Supplementary Table 1)[38].

The total rate of DIC production was assumed to be equal to the rate of DOC to DIC transformation ($R_{DIC} = R_{DOC\text{-}DIC}$). The rate of alkalinity production in the sediment was controlled by the total rate of anaerobic respiration (for example, sulfate reduction, and dissolution and precipitation of calcium carbonate. The pH depth profile in the model was obtained by using a function that calculates the different species in the carbonate system using two known dissolved species of DIC and alkalinity[14].

The stoichiometry used for organic matter degradation coupled to aerobic respiration is 1:1. This stoichiometry is based on the available literature (for example, ref. 39) that assumes that aerobic respiration in its simplest definition is the reverse of photosynthesis and the energy required to oxidize the produced organic biomass in the photic zone was initially fixed into the organic matter through photosynthesis. This is indeed a simplification for the reaction that happens in nature, as the organic matter used through aerobic respiration are large polymers that include a wide range of organic molecules such as lipids, proteins and carbohydrates. One possible representation of the chemical composition of organic matter used in aerobic respiration is the traditional Redfield–Ketchum–Richards equation, which yields a stoichiometry ratio of oxygen to organic matter of around 1.3:

$$(CH_2O)_{106}(NH_3)_{16}(H_3PO_4) + 138O_2 \rightarrow 106CO_2 + 16HNO_3 + H_3PO_4 + 122H_2O.$$

Root zone fluxes

The release of oxygen and DOC of root exudates in porewater are parameterized assuming they are dispersed in a Brownian fashion with a Gaussian probability distribution (for example, ref. 40).

$$p(j,\mu,\sigma) = \frac{1}{(2\pi\sigma^2)^{1/2}} e^{-\frac{(j-\mu)^2}{2\sigma^2}}. \quad (5)$$

Here j denotes the index for each gridpoint, μ is the gridpoint in the centre of the rootzone and 2σ regulates the number of gridpoints over which the release of oxygen and DOC happens. The release rate of oxygen and DOC at each gridpoint is calculated as:

$$R(x)_i = \frac{p(j,\mu,\sigma)F_i}{\Delta x}, \quad (6)$$

where F_i is the total flux of oxygen and DOC and Δx is the length between two consecutive gridpoints.

Boundary and initial conditions

The boundary conditions at the sediment–water interface were considered as the concentration of dissolved species (Dirichlet):

$$C_i(x=0,t) = C_i^0(t). \quad (7)$$

and imposed flux (mixed-type) for the solid species:

$$-\psi D_i(0)\frac{\partial C_i}{\partial x} + \psi u C_i = F_i(t). \quad (8)$$

Here, F_i is the solid substance flux at the sediment–water interface. A zero gradient (Neumann or second-type) no-gradient boundary condition is imposed for all species at the bottom of the domain ($x = L$):

$$\partial C_i/\partial x|_{x=L} = 0. \quad (9)$$

The initial conditions for all the species were considered zero at time zero. To explore the effect of seagrass and mangrove addition to the depth profiles of chemical species, we imposed depth profiles of chemical species in the case of no seagrass and mangroves when they reach steady state as initial conditions for the case of mangroves and seagrasses.

Surface ocean response to benthic alkalinity enhancement

A given net benthic alkalinity flux stimulated by mangrove or seagrass restoration will be imperfectly translated into an increased air–sea flux of CO_2 because of the buffering capacity of surface ocean waters[22–24,41]. To estimate the impact of this effect, we define an uptake efficiency for CO_2 removal (δCO_2) as a function of changing alkalinity (δALK)[23]:

$$\begin{aligned} &< mml_m \text{aligngroup/} > \frac{\delta CO_2}{\delta ALK} = \left[S \cdot 10^{-3.009} + 10^{-1.519}\right] \ln(pCO_2) - \left[S \cdot 10^{-2.100}\right] \\ &< mml_m \text{aligngroup/} > -[T \cdot pCO_2]\left[S \cdot 10^{-7.501} - 10^{-5.598}\right] - \left[T \cdot 10^{-2.337}\right] + 10^{-0.102}, \end{aligned} \quad (10)$$

where S and T denote in situ salinity and temperature, respectively, and pCO_2 denotes the partial pressure of atmospheric carbon dioxide (state p.p.m.). We use surface ocean temperature and salinity data from the World Ocean Atlas 2018 (ref. 42) (Supplementary Fig. 7) to estimate equilibrium uptake efficiencies for the global surface ocean (Supplementary Fig. 8). In our analysis, we apply a conservative correction to estimate rates of CO_2 removal based on benthic alkalinity enhancement ranging between 15% and 25% (for example, uptake efficiencies between 0.75 and 0.85), consistent with the observed range of uptake efficiencies for the tropical/subtropical ocean. We note, however, that these estimates assume thermodynamic equilibrium in surface seawater and gas-exchange equilibrium with the atmosphere, and thus place upper limits on effective carbon dioxide ingassing.

Reporting summary

Further information on research design is available in the Nature Portfolio Reporting Summary linked to this article.

Data availability

No dataset has been used in the study, and all the data used to produce the results of the study are from the computer code that is available through Zenodo (https://doi.org/10.5281/zenodo.7838961).

Code availability

The computer code for the time-dependent sediment diagenesis model can be found on Zenodo (DOI: 10.5281/zenodo.7838961).

References

1. Rogelj, J. et al. Scenarios towards limiting global mean temperature increase below 1.5 °C. *Nat. Clim. Change* **8**, 325–332 (2018).
2. Macreadie, P. I. et al. Blue carbon as a natural climate solution. *Nat. Rev. Earth Environ.* **2**, 826–839 (2021). *2021 2:12*.
3. Su, J., Friess, D. A. & Gasparatos, A. A meta-analysis of the ecological and economic outcomes of mangrove restoration. *Nat. Commun.* **12**, 1–13 (2021). *2021 12:1*.
4. Salem, M. E. & Mercer, D. E. The economic value of mangroves: a meta-analysis. *Sustainability* **4**, 359–383 (2012). *2012, Vol. 4, Pages 359-383*.
5. Barbier, E. B. et al. The value of estuarine and coastal ecosystem services. *Ecol. Monogr.* **81**, 169–193 (2011).
6. Krause-Jensen, D. & Duarte, C. M. Substantial role of macroalgae in marine carbon sequestration. *Nat. Geosci.* **9**, 737–742 (2016).
7. Duarte, C. M., Middelburg, J. J. & Caraco, N. Major role of marine vegetation on the oceanic carbon cycle. *Biogeosciences* **2**, 1–8 (2005).
8. van Dam, B. R. et al. Calcification-driven CO_2 emissions exceed 'Blue Carbon' sequestration in a carbonate seagrass meadow. *Sci. Adv.* **7**, 1372 (2021).
9. Reithmaier, G. M. S., Ho, D. T., Johnston, S. G. & Maher, D. T. Mangroves as a source of greenhouse gases to the atmosphere and alkalinity and dissolved carbon to the coastal ocean: a case study from the Everglades National Park, Florida. *J. Geophys. Res. Biogeosci.* **125**, e2020JG005812 (2020).
10. Saderne, V. et al. Total alkalinity production in a mangrove ecosystem reveals an overlooked Blue Carbon component. *Limnol. Oceanogr. Lett.* **6**, 61–67 (2021).

11. Saderne, V. et al. Role of carbonate burial in Blue Carbon budgets. *Nat. Commun.* **10**, 1106 (2019).
12. Burdige, D. J., Zimmerman, R. C. & Hu, X. Rates of carbonate dissolution in permeable sediments estimated from pore-water profiles: the role of sea grasses. *Limnol. Oceanogr.* **53**, 549–565 (2008).
13. Burdige, D. J., Hu, X. & Zimmerman, R. C. The widespread occurrence of coupled carbonate dissolution/reprecipitation in surface sediments on the Bahamas Bank. *Am. J. Sci.* **310**, 492–521 (2010).
14. Zeebe, R. E. & Wolf-Gladrow, D. A. *CO_2 in Seawater: Equilibrium, Kinetics, Isotopes* (Elsevier, 2001).
15. Reithmaier, G. M. S. et al. Alkalinity production coupled to pyrite formation represents an unaccounted blue carbon sink. *Glob. Biogeochem. Cycles* **35**, e2020GB006785 (2021).
16. Alongi, D. M. Lateral export and sources of subsurface dissolved carbon and alkalinity in mangroves: revising the blue carbon budget. *J. Mar. Sci. Eng.* **10**, 1916 (2022).
17. Sippo, J. Z., Maher, D. T., Tait, D. R., Holloway, C. & Santos, I. R. Are mangroves drivers or buffers of coastal acidification? Insights from alkalinity and dissolved inorganic carbon export estimates across a latitudinal transect. *Glob. Biogeochem. Cycles* **30**, 753–766 (2016).
18. Berner, R. A. *Early Diagenesis: A Theoretical Approach* (Princeton Series in Geochemistry, 1980).
19. Brodersen, K. E. et al. Oxygen consumption and sulfate reduction in vegetated coastal habitats: effects of physical disturbance. *Front Mar. Sci.* **6**, 14 (2019).
20. Zhou, Y. W., Zhao, B., Peng, Y. S. & Chen, G. Z. Influence of mangrove reforestation on heavy metal accumulation and speciation in intertidal sediments. *Mar. Pollut. Bull.* **60**, 1319–1324 (2010).
21. Stieglitz, T. C., Clark, J. F. & Hancock, G. J. The mangrove pump: the tidal flushing of animal burrows in a tropical mangrove forest determined from radionuclide budgets. *Geochim. Cosmochim. Acta* **102**, 12–22 (2013).
22. Revelle, R. & Suess, H. E. Carbon dioxide exchange between atmosphere and ocean and the question of an increase of atmospheric CO_2 during the past decades. *Tellus* **9**, 18–27 (1957).
23. Renforth, P. & Henderson, G. Assessing ocean alkalinity for carbon sequestration. *Rev. Geophys.* **55**, 636–674 (2017).
24. Egleston, E. S., Sabine, C. L. & Morel, F. M. M. Revelle revisited: buffer factors that quantify the response of ocean chemistry to changes in DIC and alkalinity. *Glob. Biogeochem. Cycles* https://doi.org/10.1029/2008GB003407 (2010).
25. Carbon dioxide capture and storage. *IPCC* https://www.ipcc.ch/report/carbon-dioxide-capture-and-storage/
26. Rosentreter, J. A., Al-Haj, A. N., Fulweiler, R. W. & Williamson, P. Methane and nitrous oxide emissions complicate coastal blue carbon assessments. *Glob. Biogeochem. Cycles* **35**, e2020GB006858 (2021).
27. Chauhan, R., Ramanathan, A. L. & Adhya, T. K. Assessment of methane and nitrous oxide flux from mangroves along Eastern coast of India. *Geofluids* **8**, 321–332 (2008).
28. Muoz-Hincapié, M., Morell, J. M. & Corredor, J. E. Increase of nitrous oxide flux to the atmosphere upon nitrogen addition to red mangroves sediments. *Mar. Pollut. Bull.* **44**, 992–996 (2002).
29. Corredor, J. E., Morell, J. M. & Bauza, J. Atmospheric nitrous oxide fluxes from mangrove sediments. *Mar. Pollut. Bull.* **38**, 473–478 (1999).
30. Middelburg, J. J., Soetaert, K. & Hagens, M. Ocean alkalinity, buffering and biogeochemical processes. *Rev. Geophys.* **58**, e2019RG000681 (2020).
31. Bayraktarov, E. et al. The cost and feasibility of marine coastal restoration. *Ecol. Appl.* **26**, 1055–1074 (2016).
32. Tan, Y. M. et al. Seagrass restoration is possible: insights and lessons from Australia and New Zealand. *Front Mar. Sci.* **7**, 617 (2020).
33. Strefler, J. et al. Carbon dioxide removal technologies are not born equal. *Environ. Res. Lett.* **16**, 074021 (2021).
34. Meadowcroft, J. Exploring negative territory carbon dioxide removal and climate policy initiatives. *Clim. Change* **118**, 137–149 (2013).
35. National Academies of Sciences, Engineering, and Medicine et al. *Negative Emissions Technologies and Reliable Sequestration: A Research Agenda* (National Academies Press, 2018).
36. Middelburg, J. J. A simple rate model for organic matter decomposition in marine sediments. *Geochim. Cosmochim. Acta* **53**, 1577–1581 (1989).
37. Katsev, S. & Crowe, S. A. Organic carbon burial efficiencies in sediments: the power law of mineralization revisited. *Geology* **43**, 607–610 (2015).
38. Wilson, J. D. & Arndt, S. Modeling radiocarbon constraints on the dilution of dissolved organic carbon in the deep ocean. *Glob. Biogeochem. Cycles* https://doi.org/10.1002/2016GB005520 (2017).
39. Burdige, D. J. *Geochemistry of Marine Sediments* (Princeton Univ. Press, 2007).
40. Eldridge, P. M. & Morse, J. W. A diagenetic model for sediment–seagrass interactions. *Mar. Chem.* **70**, 89–103 (2000).
41. Frankignoulle, M. A complete set of buffer factors for acid/base CO_2 system in seawater. *J. Mar. Syst.* **5**, 111–118 (1994).
42. World Ocean Atlas 2018. *National Centers for Environmental Information* https://www.ncei.noaa.gov/access/metadata/landing-page/bin/iso?id=gov.noaa.nodc:NCEI-WOA18 (2018).

Acknowledgments

N.J.P. acknowledges funding from the David and Lucile Packard Foundation and the Yale Center for Natural Carbon Capture. C.T.R. acknowledges support from a Cullen-Peck Scholar Award from the Georgia Institute of Technology.

Author contributions

Conceptualization: N.J.P., M.F. and C.T.R. Methodology: M.F., N.J.P. and C.T.R. Investigation: M.F., N.J.P. and C.T.R. Visualization: M.F., N.J.P. and C.T.R. Funding acquisition: N.J.P. and C.T.R. Project administration: N.J.P. and C.T.R. Supervision: N.J.P. and C.T.R. Writing—original draft: M.F., N.J.P. and C.T.R. Writing—review and editing: M.F., N.J.P. and C.T.R.

Competing interests

The authors declare no competing interests.

Additional information

Supplementary information The online version contains supplementary material available at https://doi.org/10.1038/s41893-023-01128-2.

Correspondence and requests for materials should be addressed to Mojtaba Fakhraee or Noah J. Planavsky.

Peer review information *Nature Sustainability* thanks Lucy Gwen Gillis, Gloria Reithmaier and the other, anonymous, reviewer(s) for their contribution to the peer review of this work.

Corresponding author(s): Mojtaba Fakhraee; Noah J. Planavsky
mojtaba.fakhraee@yale.edu;
noah.planavsky@yale.edu

Last updated by author(s): Mar 27, 2023

Reporting Summary

Nature Portfolio wishes to improve the reproducibility of the work that we publish. This form provides structure for consistency and transparency in reporting. For further information on Nature Portfolio policies, see our Editorial Policies and the Editorial Policy Checklist.

Statistics

For all statistical analyses, confirm that the following items are present in the figure legend, table legend, main text, or Methods section.

n/a	Confirmed
☐	☒ The exact sample size (*n*) for each experimental group/condition, given as a discrete number and unit of measurement
☒	☐ A statement on whether measurements were taken from distinct samples or whether the same sample was measured repeatedly
☒	☐ The statistical test(s) used AND whether they are one- or two-sided *Only common tests should be described solely by name; describe more complex techniques in the Methods section.*
☒	☐ A description of all covariates tested
☒	☐ A description of any assumptions or corrections, such as tests of normality and adjustment for multiple comparisons
☒	☐ A full description of the statistical parameters including central tendency (e.g. means) or other basic estimates (e.g. regression coefficient) AND variation (e.g. standard deviation) or associated estimates of uncertainty (e.g. confidence intervals)
☒	☐ For null hypothesis testing, the test statistic (e.g. *F*, *t*, *r*) with confidence intervals, effect sizes, degrees of freedom and *P* value noted *Give P values as exact values whenever suitable.*
☒	☐ For Bayesian analysis, information on the choice of priors and Markov chain Monte Carlo settings
☒	☐ For hierarchical and complex designs, identification of the appropriate level for tests and full reporting of outcomes
☒	☐ Estimates of effect sizes (e.g. Cohen's *d*, Pearson's *r*), indicating how they were calculated

Our web collection on statistics for biologists contains articles on many of the points above.

Software and code

Policy information about availability of computer code

Data collection	A computer code built in Matlab was used to generate the results of the study.
Data analysis	A computer code built in Matlab was used to generate the results of the study.

For manuscripts utilizing custom algorithms or software that are central to the research but not yet described in published literature, software must be made available to editors and reviewers. We strongly encourage code deposition in a community repository (e.g. GitHub). See the Nature Portfolio guidelines for submitting code & software for further information.

Data

Policy information about availability of data

All manuscripts must include a data availability statement. This statement should provide the following information, where applicable:

- Accession codes, unique identifiers, or web links for publicly available datasets
- A description of any restrictions on data availability
- For clinical datasets or third party data, please ensure that the statement adheres to our policy

All model code and configuration files will be made available
by request following the publication.

Human research participants

Policy information about studies involving human research participants and Sex and Gender in Research.

Reporting on sex and gender	NA
Population characteristics	NA
Recruitment	NA
Ethics oversight	NA

Note that full information on the approval of the study protocol must also be provided in the manuscript.

Field-specific reporting

Please select the one below that is the best fit for your research. If you are not sure, read the appropriate sections before making your selection.

☐ Life sciences ☐ Behavioural & social sciences ☒ Ecological, evolutionary & environmental sciences

For a reference copy of the document with all sections, see nature.com/documents/nr-reporting-summary-flat.pdf

Ecological, evolutionary & environmental sciences study design

All studies must disclose on these points even when the disclosure is negative.

Study description	Our study investigate the role of coastal habitats in increasing the flux of alkalinity from the sediment and thereby reducing the concentration of carbon dioxide in the atmosphere.
Research sample	We used a computation model built in Matlab to generate the results presented in the study.
Sampling strategy	NA
Data collection	NA
Timing and spatial scale	NA
Data exclusions	NA
Reproducibility	The computer code used to generate the results will be available upon the request from the corresponding authors of the study.
Randomization	NA
Blinding	NA

Did the study involve field work? ☐ Yes ☒ No

Reporting for specific materials, systems and methods

We require information from authors about some types of materials, experimental systems and methods used in many studies. Here, indicate whether each material, system or method listed is relevant to your study. If you are not sure if a list item applies to your research, read the appropriate section before selecting a response.

Materials & experimental systems

n/a	Involved in the study
☒	☐ Antibodies
☒	☐ Eukaryotic cell lines
☒	☐ Palaeontology and archaeology
☒	☐ Animals and other organisms
☒	☐ Clinical data
☒	☐ Dual use research of concern

Methods

n/a	Involved in the study
☒	☐ ChIP-seq
☒	☐ Flow cytometry
☒	☐ MRI-based neuroimaging